# LANGMUIR

pubs.acs.org/Langmuir Article

# Splashing on Soft Elastic Substrates

Bailey C. Basso and Joshua B. Bostwick\*



Cite This: https://dx.doi.org/10.1021/acs.langmuir.0c02500

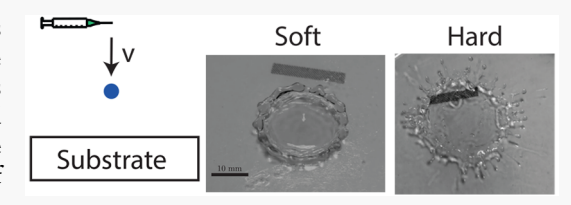


**ACCESS** 

Metrics & More

Article Recommendations

**ABSTRACT:** Drop impact onto soft substrates is important in applications such as bioprinting, spray coating, and aerosol drug delivery. Experiments are conducted to determine the effect of elasticity on the splash morphology, as defined by the splashing threshold, spine number, spreading factor, and retraction factor. PDMS silicone gel and gelatin hydrogel are used as the substrates because they have different wetting properties and a large range of elasticities. The splash threshold, as defined by the Weber number *We*,



increases as the substrate elasticity decreases indicating that it is harder to splash on soft substrates. After impact, the drop spreads to a maximum diameter that decreases for soft substrates, irrespective of wetting properties, illustrating the role of substrate deformation in the energy balance during splashing. The number of spines that form at the leading edge of the drop depends upon the elasticity and the wetting properties of the liquid/substrate system. Following spreading, the drop retracts to an equilibrium diameter which does not show a strong correlation with any material properties. The reported results agree well with the existing literature for most cases and also provide new insights into gels with small elasticity.

# **■ INTRODUCTION**

Droplet splashing has fascinated scientists since the late 19th century when Worthington first illuminated a splash at the moment of impact.¹ Recent technological advances in high-speed imaging have made it possible to reveal a number of different splash morphologies. As such, there is a large volume of literature devoted to the study of splashing on liquids baths and rigid substrates, which describe how the impact dynamics are affected by liquid properties, e.g., surface tension,² density,³ and viscosity,⁴ and substrates properties, e.g., wettability,⁵ texture/micropatterning,⁶ and stiffness,⁻-9 as well as the ambient air pressure.¹ Somewhat surprising given the vast literature is that splashing on soft substrates has been comparatively unexplored. This is the focus of this paper.

Droplet impact onto soft substrates is seen in many industrial applications and technologies. For example, bioprinting technologies utilize similar techniques to inkjket printing 11,12 but adapted for living cells. Tissue scaffolds are built by depositing drops onto soft substrates to manufacture organs, for example, and quality control is an issue. Similarly, aerosol drug delivery in the lungs involves drop deposition onto soft tissues and the efficiency of drug delivery is related to the impact dynamics. This is also important to quantify the spread of infectious disease that attaches to the lungs via aerosols.<sup>13</sup> In both such applications, the tissue can be viewed as a soft elastic substrate. Blood splatter analysis has also been used to recreate crime scenes by interpreting the spread and morphology of the drop impact, and these characteristics are affected by the substrate properties.<sup>14</sup> In this paper, we quantify the drop impact dynamics on soft elastic substrates to aide in improving the aforementioned applications.

Investigation into the influence of substrate elasticity on droplet impact was studied by Rioboo et al. 15 who showed that contact angle hysteresis was prominent on elastomer substrates and that hysteresis was a function of the impact velocity which influenced the size of substrate deformation. Later, Chen and Li<sup>16</sup> showed that drops could fully rebound off soft substrates provided the elasticity  $E \sim 4$  kPa. They hypothesized the mechanism of full rebound is the formation of an air film at the interface due to the deformation of the substrate. 17 Substrate elasticity has been shown to provide little effect on the spreading stage of an impacting droplet while greatly affecting the receding phase. Carré et al. first described the viscoelastic dissipation retarding force that affects the receding phase so greatly. For reference, the maximum surface deformation was observed to be on the order of 10  $\mu$ m for a substrate with an elasticity  $E \approx 17$  kPa. <sup>19</sup> The first study to determine if soft substrates could absorb impact energy and suppress splashing was done by Howland et al.,20 who investigated gels with elasticity in the range of 5-500 kPa and showed that impacts on their softest substrates required 70% more kinetic energy to splash than on rigid substrates. This suppression of splashing is explained by the removal of energy from the ejecta sheet not from the bulk of the liquid droplet. With the ejecta sheet having less energy, it is harder

Received: August 23, 2020 Revised: October 19, 2020



for it to break up, and therefore a prompt splash is avoided. More recently work has been done to confirm the ability for soft substrates to suppress splashing by controlling the tension of the membrane to effectively change the elasticity. Here decreasing the substrate elasticity increases the splashing threshold.

Drop impact creates numerous splash morphologies. On liquid substrates, microdroplets are the first to be observed after impact, followed by the Peregrine sheet which rises up from the liquid bath that can then turn into a crown splash which can break up into secondary droplets if the initial inertia of the droplet is high enough. As the drop retracts, a Rayleigh jet can form and again if the inertia of the jet is high enough the jet can break up into droplets.<sup>21</sup> The manner in which a droplet splashes during an impact with a liquid surface is reliant on the production of two different sheets. The first being the ejecta sheet, formed at the moment of impact, which was first observed experimentally by Thoroddsen.<sup>22</sup> Here a pressure singularity forms at the contact point when the drop impacts the surface which pushes fluid outward. The speed at which the ejecta sheet shoots out has been measured to be as high as 50 m/s. <sup>22</sup> Surface tension can slow the ejecta sheet, and Weiss and Yarin <sup>23</sup> showed that for a Weber number We < 40, no ejecta sheet was produced. It is thought that secondary droplets which appear before a crown splash has formed are due to the breakup of the ejecta sheet.<sup>24</sup> Once the drop has penetrated the fluid layer, the Peregrine sheet forms<sup>25</sup> and is what carries the leading edge or the rim that has the ability to become fingerlike which can lead to instability and the formation of secondary droplets. At low impact velocities, a thin layer of air can become trapped between the droplet and the liquid bath. This air pocket will breakdown to form a chandelier of bubbles known as Mesler entrainment.<sup>26</sup> On solid substrates, drop impact leads to bouncing, spreading, and splashing, and these generally depend upon the impact velocity, liquid properties, and surface wettability.<sup>27</sup> By simply changing the wetting contact angle, Lin et al. 28 observed deposition (spreading), partial rebound, full rebound, and bubble entrapment on both the surface and the droplet, and splashing. When a droplet first impacts a solid substrate, it is likely to result in a prompt splash.<sup>29</sup> That is, liquid is ejected diagonally away from the contact line between the drop and the solid substrate.<sup>30</sup> These droplets form at the tip of the lamella at high speeds and is known to happen within the first 10  $\mu$ s.<sup>31</sup> The other type of splashing on solid substrates is a corona splash, which is also seen on liquid substrates.<sup>30</sup> The corona splash occurs later during the impact and can be described as droplets forming around the rim of the corona.<sup>3</sup> During a corona splash the lamella, still intact, separates from the solid surface and eventually reaches a bowl shape with droplets ejecting from its fingerlike structures.<sup>31</sup> For soft substrates, it is reasonable to assume that the splash morphology exhibits characteristics similar to both liquid and solid substrates. In particular, we are interested in the splash threshold, spine number N, spreading factor  $\alpha$ , and retraction factor  $\beta$ .

We begin this paper by describing the experimental setup and protocols to study drop impact on soft PDMS silicone and gelatin hydrogel substrates focusing on the role of substrate elasticity which ranges from  $E=0.51-47\,$  kPa for our experiments. Two working liquids are used, deionized water and ethanol, which exhibit different wetting properties on the respective substrates. High-speed imaging is used to quantify

the splash morphology through the splash threshold defined by the Weber number We, spine number N, spreading factor  $\alpha$ , and retraction factor  $\beta$ , as they depend upon the experimental parameters. For soft substrates, decreasing the substrate elasticity tends to increase the splashing threshold and decrease droplet spreading. The formation of spines has a more complicated dependence on the elasticity as well as the wetting properties of the liquid/substrate system. We conclude by offering some remarks on the relevance of our study to industrial and technological applications.

#### EXPERIMENT

Experiments are performed by impacting millimeter-sized droplets onto soft substrates using the experimental apparatus shown in Figure 1. High-speed imaging is used to quantify the splash dynamics, as it depends upon the elasticity and wetting properties of the substrate.

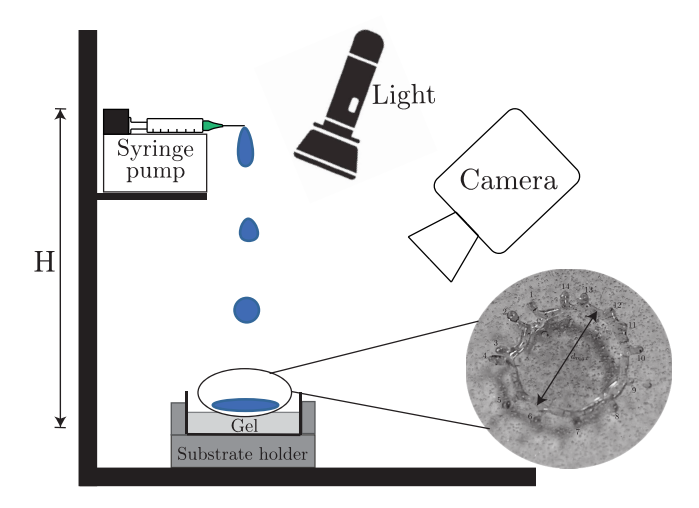


Figure 1. Experimental setup.

Deionized water and ethanol are used as the working liquid with materials properties: density  $\rho$ , viscosity  $\eta$ , and surface tension  $\sigma$  given in Table 1, with the density measured by an

Table 1. Liquid Properties

fluid	viscosity $\eta$ [mm <sup>2</sup> /s]	density $ ho$ [kg/m $^3$ ]	surface tension $\sigma$ [mN/m]
water	1.0	980	71.6
ethanol	1.37	760	22.1

Anton-Paar DMA 35 density meter, viscosity by an Anton-Paar MCR-302 rheometer, and surface tension by a NanoScience Sigma 702-D tensiometer. Drops are formed using a syringe pump with a needle diameter of 0.69 mm set at a low flow rate, such that drops pinch off of the needle due to surface tension in a quasi-static manner. This protocol gives repeatable-sized water drops of diameter d=3.6 mm and ethanol drops with d=3.2 mm. The syringe pump is located at a height H above the substrate that ranges from H=0.12-0.80m. The falling drop impacts the substrate with velocity v=1.5-3.9 m/s. This gives a Weber number  $We \equiv \rho v^2 d/\sigma = 100-1800$  and Reynolds number  $Re \equiv v d/\eta = 3500-14000$ , which is a measure of drop inertia to surface tension and viscous forces, respectively.

Two types of substrates are used in the experiment: PDMS silicone gel and gelatin hydrogel. Silicone gels are comprised of

Figure 2. A drop of diameter d impacts a soft substrate, spreads to a maximum diameter  $d_{\text{max}}$  and then retracts to a final diameter  $d_{\text{final}}$ .

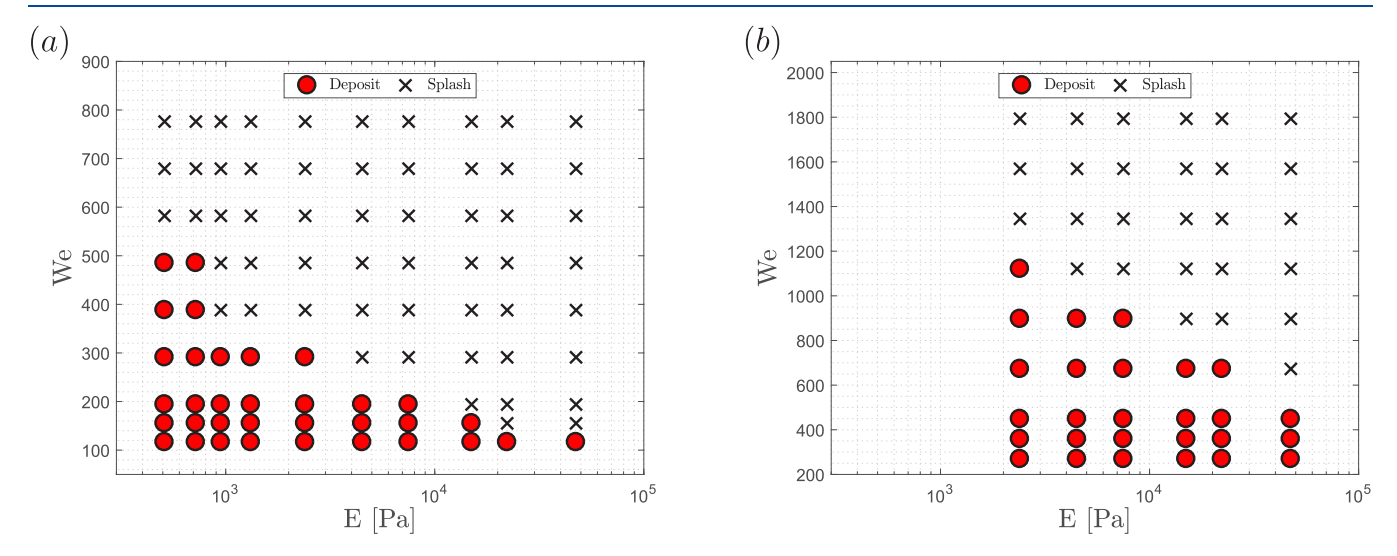


**Figure 3.** Phase diagram plotting the Weber number *We* against the substrate elasticity *E* for (a) water and (b) ethanol showing regions of drop deposition and splashing. Note the different *y*-axis scales in the subplots.

a base (Gelest DMS-V31), cross-linker (Gelest HMS-301), and catalyst (Gelest SIP6831.2). The catalyzed base and crosslinker are mixed in a prescribed ratio, cast into a Petri dish with an inner diameter of 60 mm, and baked in an oven at 63 °C for 6 h until gelled. Gelatin hydrogel is made by dissolving bovine powder (Sigma-Aldrich G9382) into deionized water at 70 °C. The mixture is stirred for 60 min and then poured into a Petri dish, covered to avoid evaporation, and left overnight to gel. The thickness of the gels was  $7 \pm 2$  mm. Both gels are considered incompressible with a Poisson ratio  $\nu = 1/2$ .<sup>33</sup> The elasticity E of the gels was measured using an oscillatory test on a Anton-Paar MCR302 rheometer. The range of elasticity explored for silicone gels was E = 4.5-47 kPa and for gelating hydrogels was E = 0.52-7 kPa. More details about how the substrate elasticity depends upon the mixing ratios are given in the Substrate Properties. The static contact angle  $\theta$  for deionized water and ethanol on silicone gel is 89° and 30°, respectively, and on gelatin hydrogel is 105° and 45°,

Drop impact is captured using a Phantom VEO 410L high-speed camera at 5200 fps. Each experiment is repeated 5 times to ensure repeatability, and we report the average of that data with 95% confidence intervals as error bars. A typical drop impact is illustrated in Figure 2. The drop impacts and spreads on the substrate to a maximum diameter  $d_{\rm max}$  at which point a number of spines N may form as an instability of the leading edge of the rim. The drop then retracts to an equilibrium diameter  $d_{\rm final}$ . In general, these shapes are irregular and the length  $d_{\rm max}/d_{\rm min}$  reported is the average of four measurements taken across the drop. We quantify the splash dynamics through the dimensionless variables by scaling lengths with the

initial drop diameter d; spine number N, spreading factor  $\alpha \equiv d_{\max}/d$ , and retraction factor  $\beta \equiv d_{\text{final}}/d$ .

# ■ RESULTS AND DISCUSSION

In this section, we experimentally quantify the splashing threshold, spine number, spreading factor, and retraction factor, as they depend upon the liquid properties, drop impact velocity, and substrate elasticity. The focus here is on soft substrates. For reference, we use acrylic E=3.2 GPa as a proxy for what we will refer to as a "hard substrate", which has an elasticity many orders of magnitude higher than the gels used here.

Splashing. During a given experiment, the simplest observation is whether the drop (i) splashes or (ii) deposits on the substrate. This distinction is important in many inkjet printing applications as splashing is undesirable from a quality control perspective. We define a "splash" as either (i) a drop that produces microdroplets immediately after impact or (ii) a drop that exhibits two or more satellite drops that break off from the fingers that extend off of the main drop during impact. Splashing typically occurs when the liquid inertia overcomes the surface tension forces. As such, splashing is typically quantified by the Weber number We. On soft substrates, one might expect that some of the liquid energy can be transmitted into the elastic energy of substrate deformation, therefore affecting the impact dynamics and the ability to splash. This is illustrated in the phase diagrams shown in Figure 3, which plots the Weber number We against the substrate elasticity E defining regions of splashing and deposition. For each elasticity E, splashing occurs for a range of Weber numbers indicative that a given drop inertia is required

to produce a splash. For soft substrates (lower *E*), a higher *We* is required to produce a splash, indicating that it is harder to splash on soft substrates (Figure 4). Note that each marker is an average of five trials, as such the closer to the splashing threshold, the more statistical uncertainty.

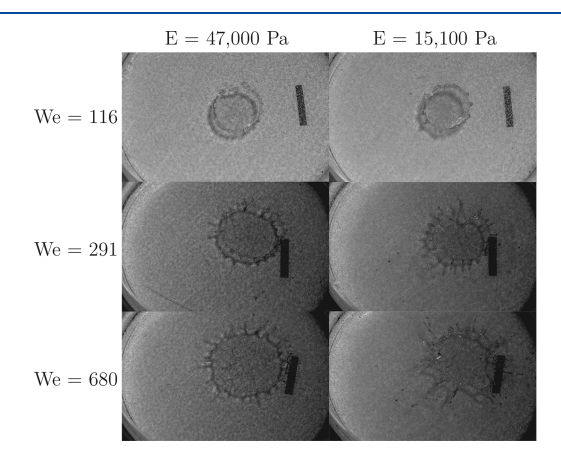


**Figure 4.** Typical images of drop impact for water on PDMS silicone gels, as it depends upon elasticity *E* and Weber number *We*.

Even though the phase diagrams for water and ethanol appear qualitatively similar, they are not quantitatively similar as evident by the difference in the vertical scale (cf. Figure 3). Work by Mundo et al.<sup>34</sup> have suggested the dimensionless number  $K = Re^{1/4}We^{1/2}$  as an effective metric to quantify splashing, and we attempt to collapse all of our data in the phase diagram shown in Figure 5, which plots K against E. The

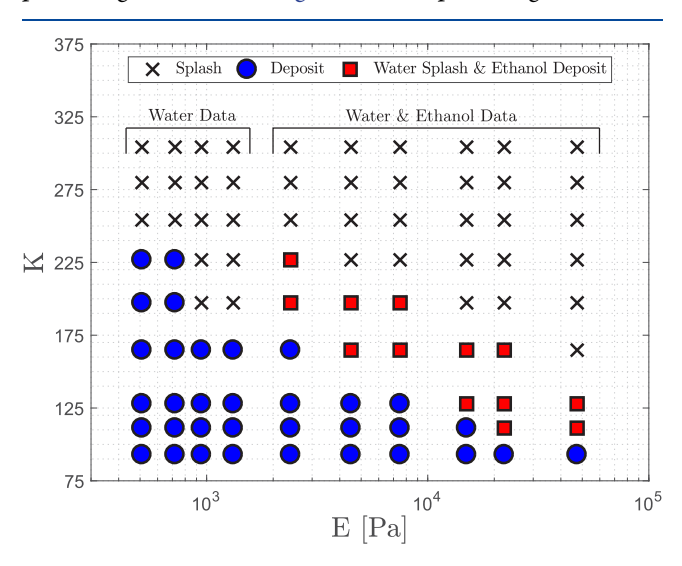


**Figure 5.** Combined phase diagram plotting the nondimensional parameter  $K = Re^{1/4}We^{1/2}$  against elasticity E showing regions of splashing, deposition, and an overlap region where water splashes but ethanol deposits.

collapse is reasonable with the exception of the small overlap region where water splashes and ethanol deposits. Here ethanol consistently displays a higher splashing threshold relative to water, which we attribute to increased viscosity that slows the eject sheet thus suppressing splashing, as well as the different wetting properties, i.e., ethanol tends to better wet the gel substrates than water. Our results agree well with Howland et al.<sup>20</sup> in that soft substrates have a much higher splashing

threshold than hard substrates, and we have quantified this for multiple liquids and multiple gel substrates. Our work is distinguished in that we explore much softer gels with elasticity as low as E=510 Pa. This is approaching a lower bound for our splashing experiments, as it is well-known that drops can cause starburst fractures on ultrasoft gels ( $E\approx50$  Pa).

**Spine Number.** Splashes and depositions are typically preceded by the formation of spines at the rim of the spreading drop. Figure 6 plots the spine number N against Weber number We for water and ethanol. The spine number increases monotonically with N, as could be expected. For water, the spine number N increases with substrate elasticity E for all We, with the largest spine number occurring for the acrylic substrate (E = 3.2 GPa) and smallest spine number for our softest hydrogel (E = 510 Pa). In contrast, the trend with elasticity for ethanol is opposite to that of water with the lowest spine number corresponding to the acrylic substrate. We attribute this observation to the inherent difference in wetting properties of water and ethanol. To explain, the formation of spines is related to a competition between inertia (spreading) and surface tension (wetting). During drop impact, the initial kinetic energy can be transformed via spreading or shape change (i.e., spine formation). For ethanol, the wetting force acts in the direction of the spreading drop and assists spreading, but for water it is in the opposite direction and resists spreading. Accordingly, it is reasonable to assume the energy balance favors spreading for ethanol but spine formation for water. For soft substrates, the energy of elastic deformation increases with decreasing E and this energy is taken from either droplet spreading or shape change. This energy balance leads to the trends with elasticity shown in Figure 6.

**Spreading Factor.** Figure 7 plots the spreading factor  $\alpha$ against the Weber number We showing an increasing trend with We for each liquid/substrate pair. For water, the softest gel E = 510 Pa has the lowest spreading factor, and the stiffest substrate acrylic with E = 3.2 GPa has the highest spreading factor, indicating that soft substrates inhibit the droplet spreading after impact. This is contrary to the previous literature that reports substrate elasticity has little effect on the spreading factor for droplet impact.<sup>39'</sup> Although it has been shown that soft substrates yield small deformations during droplet impact, it has been postulated that these deformations are sufficiently small such that the elastic energy of deformation does not markedly affect spreading or splashing.<sup>20</sup> Our experiments are distinguished in that we use gels with smaller elasticity such that the elastic deformations are nontrivial and do affect the spreading factor. This can be seen for water when  $E \le 1.3$  kPa and for ethanol when  $E \le 7$ kPa. For ethanol, it is interesting that hydrogel and silicone gel data tend to cluster together, and this illustrates that wetting properties play a significant role in droplet spreading during impact. Both liquids have maximum spreading factor on the stiffest acrylic substrate.

Figure 8 plots the spreading factor for all of our data against the Weber number We, with water and ethanol represented by the blue and red symbols, respectively. In general, our data collapses well with the exception of the softest substrates. For water, the data collapses to the scaling given by  $\alpha \sim We^{1/4}$ , which agrees well with Roisman, 40 and for ethanol the best fit is given by  $\alpha \sim We^{1/10}$ , but the spread is admittedly large. These different trends are presumably due to the differing liquid properties and can be linked to the different surface

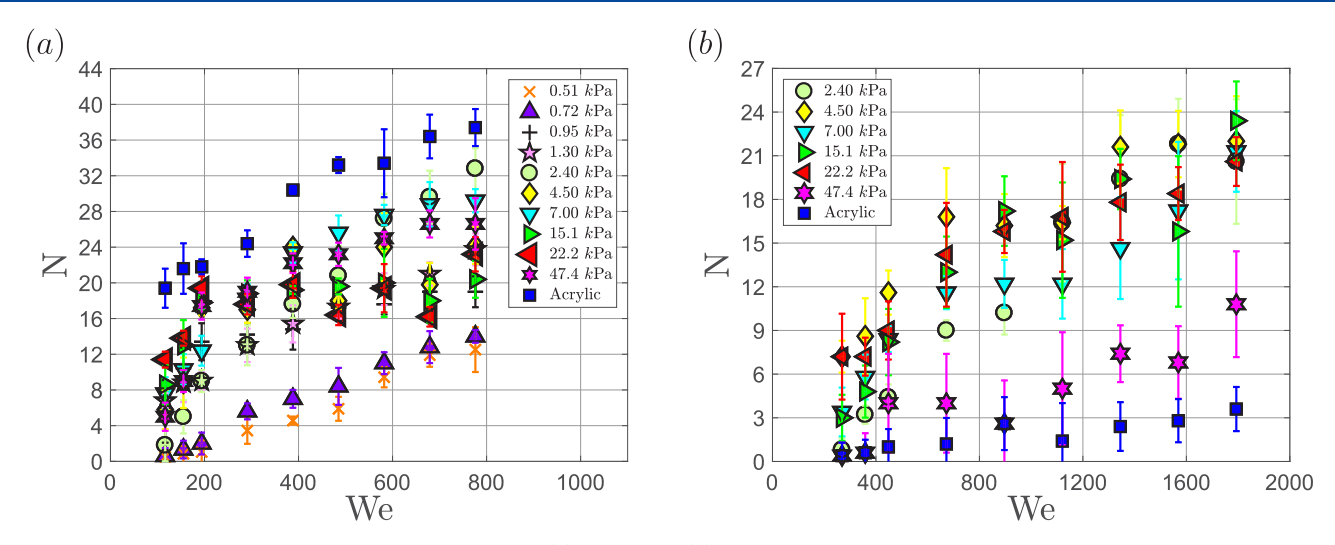


Figure 6. Spine number N against Weber number We for (a) water and (b) ethanol. Error bars are 95% confidence intervals.

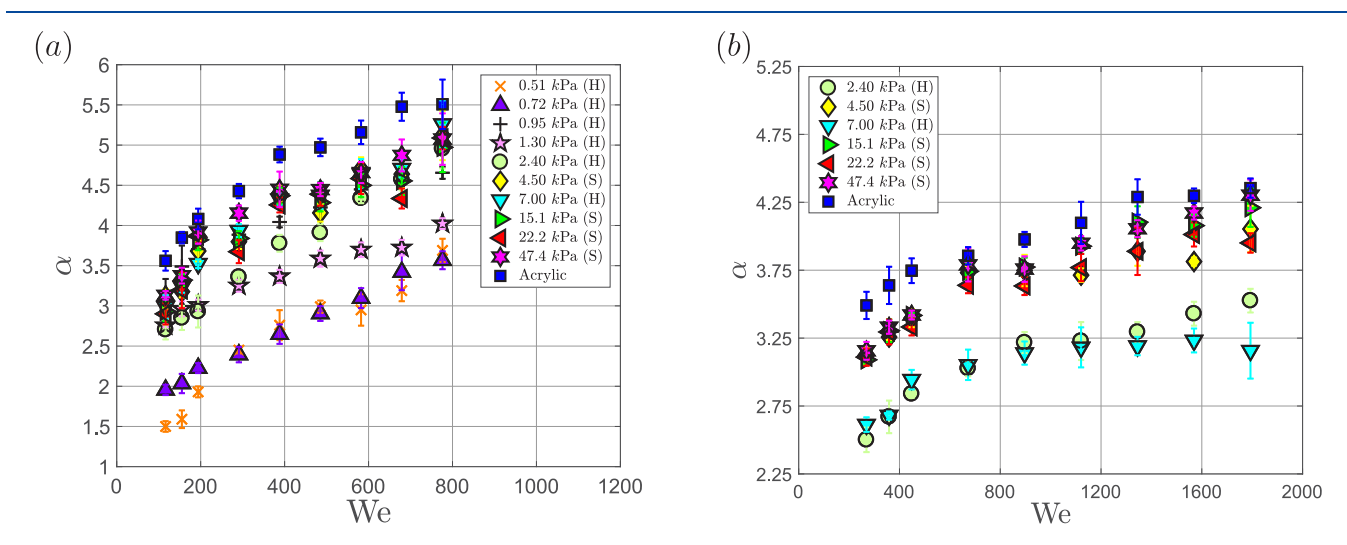
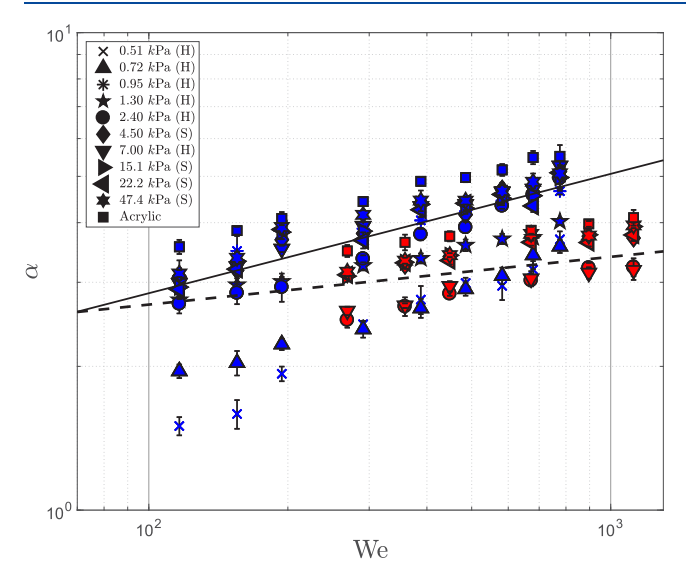


Figure 7. Spreading factor  $\alpha$  against Weber number We for (a) water and (b) ethanol. Error bars are 95% confidence intervals.



**Figure 8.** Spreading factor  $\alpha$  against Weber number We for all data. Solid trendline is  $\alpha \sim We^{1/4}$ . Dashed trendline correspond to  $\alpha \sim We^{1/10}$ . Water and ethanol are represented by blue and red symbols, respectively.

tension and viscosity values. Despite these discrepancies, we do show very good agreement with Andrade et al. 41 who show that for low viscosity liquids the spreading factor scales by  $\alpha \sim We^{0.25\pm0.02}$  and for higher viscosity liquids the spreading factor scales by  $\alpha \sim We^{0.16\pm0.02}$ . As previously discussed, our data does not collapse for either liquid on the softest substrates indicating that elasticity plays a role in governing the spreading dynamics.

Retraction Factor. Following spreading, the drop retracts from its maximum diameter due to surface tension effects and equilibrates at its final diameter. We plot the retraction factor  $\beta$ against the Weber number We in Figure 9. Recall that a smaller  $\beta$  means the drop retracts more. In general, the trend with We is weak, and for water  $\beta$  is almost independent of We. There is a clear distinction between the hydrogel and silicone gel substrates; silicone gels have lower  $\beta$ , meaning they retract more than the hydrogels. For water, there is generally no trend with elasticity, but we note the E = 7 kPa hydrogel has a relatively large  $\beta$  and may be an outlier in our data. There is a slight trend for the ethanol/silicone gel system which shows the retraction factor increases with for soft substrates, i.e., decreasing elasticity. This agrees well with the literature in which the final diameter increases with decreasing stiffness.7 This observation is related to the substrate deformation at the

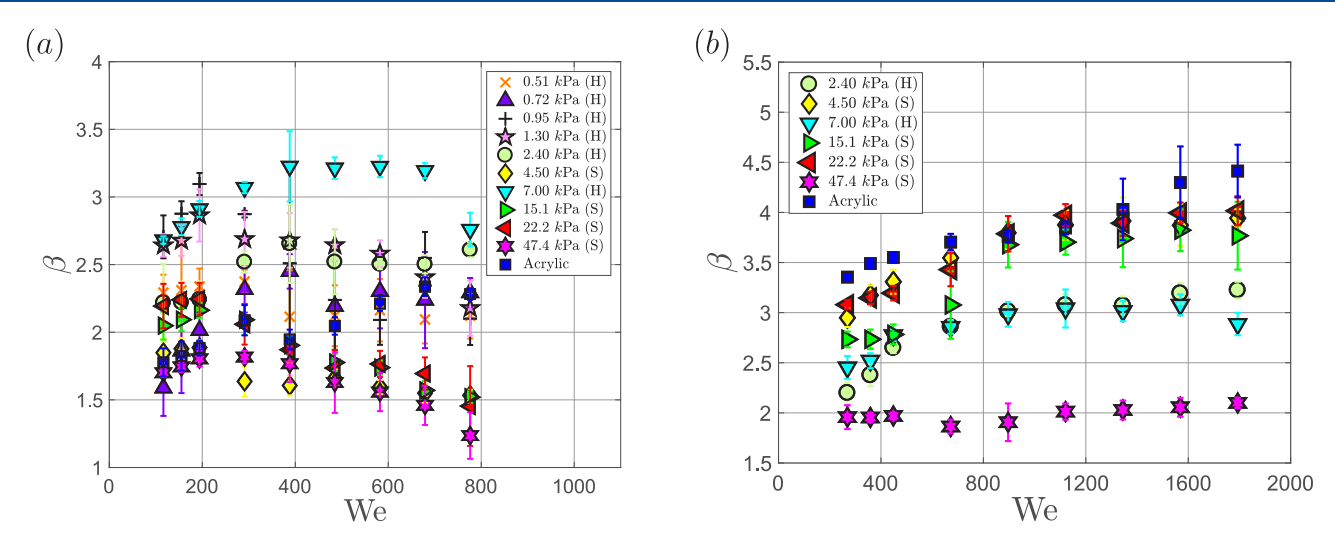


Figure 9. Retraction factor  $\beta$  against Weber number We for (a) water and (b) ethanol. Error bars are 95% confidence intervals.

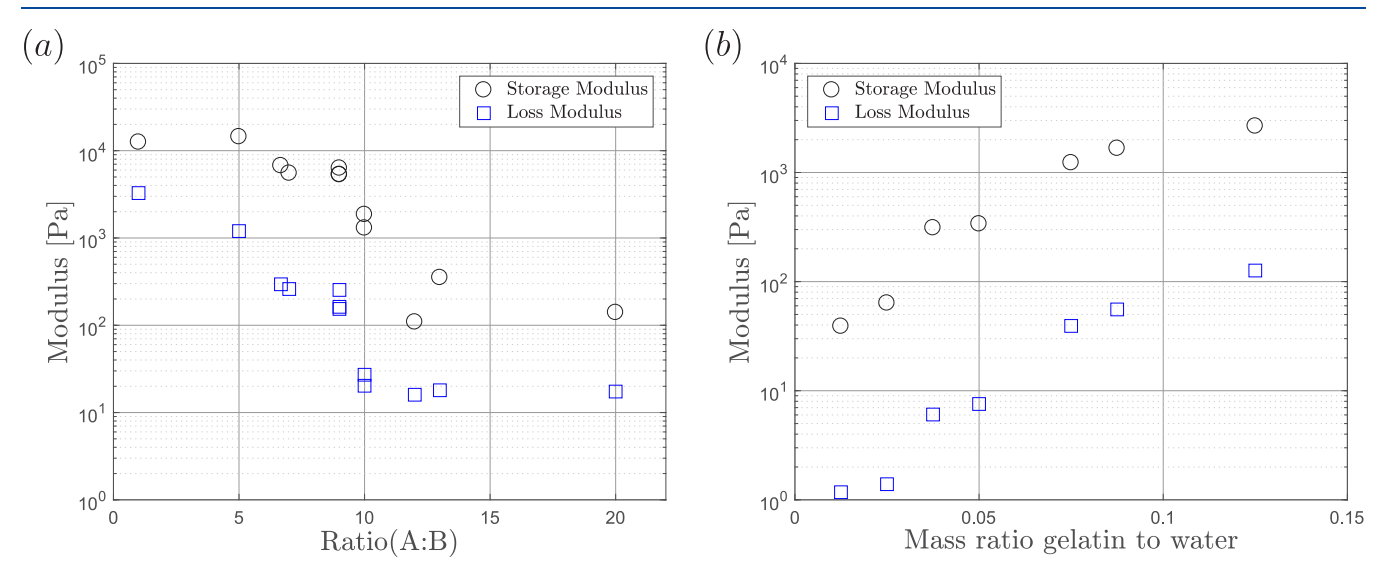


Figure 10. Storage modulus and loss modulus against (a) ratio of base to cross-linker (A:B) for PDMS silicone gels and (b) mass ratio of gelatin powder to DI water for hydrogels.

three-phase contact line, which causes dissipation to fluid motion thereby reducing the contact-line velocity of the receding droplet.<sup>39</sup> Our experimental data for drop retraction is somewhat scattered, and a more detailed study of the retraction dynamics should be pursued.

Wetting Effects. These results have demonstrated how substrate elasticity affects the splashing dynamics during drop impact. In addition to elasticity, liquid/substrate wettability plays a large role in spine formation  $N_i$ , droplet spreading  $\alpha_i$ and drop retraction  $\beta$ . Previous literature has shown that when comparing substrates, high wettability favors liquid displacement and the suppression of spine formation in spreading droplets. 42 We see this phenomena in Figure 6, which plots the spine number N against the Weber number We, and shows lower N for substrates with higher wettability. Wetting can also explain the grouping of ethanol data in Figure 7 by substrate type, hydrogel or silicone gel, which each have unique wetting properties. We note that for soft substrates, wetting is more complicated due to the elastic deformation at the contact-line, and this has been shown for both static and dynamic wetting. 43-45 In general, droplet retraction is most affected

by wettability, e.g., Bayer and Megaridis<sup>46</sup> have shown that wettable surfaces see only slight retraction when compared to surfaces with lower amounts of wettability. This is attributed to two main effects: (1) the smaller contact angle causes lower retraction speeds, consistent with dynamic wetting effects, <sup>47–49</sup> and (2) contact-line pinning has been shown to suppress droplet retraction on highly wettable substrates. <sup>50</sup> These effects have been shown for hard substrates, and it is reasonable to expect that the physics of droplet spreading and retraction become more complicated on soft substrates due to elastic deformation. This should be explored further.

# CONCLUDING REMARKS

An experimental investigation of droplet splashing on soft substrates has been performed from which we have quantified the splash morphology by the spine number N, spreading factor  $\alpha$ , and retraction factor  $\beta$ . We report the splashing threshold, as it depends upon the substrate elasticity, for multiple soft elastic substrates and various liquids showing that it is harder to splash on soft substrates. Furthermore, we show that drop spreading decreases for soft substrates. Both of these

observations illustrate the critical role of substrate deformation in the energy balance during drop impact. Interestingly, we also show that wetting effects are important in the formation of spines at the leading edge of the spreading drop and that the trend with elasticity is opposite for water and ethanol, which exhibit neutral and hydrophilic wetting properties on our soft substrates, respectively. The retraction dynamics do not illustrate a consistent trend and should be explored further.

Our work can provide new insights into numerous technologies that involve the interactions of liquids on soft solids, such as bioprinting, aerosol drug delivery, and pesticide application. For example, Figure 3 presents a phase diagram to quantify the splashing threshold which can predict the highest drop impact velocity for deposition for a substrate with a given elasticity. This is useful for quality control purposes in tissue engineering applications which involve drop deposition onto soft substrates and also for optimization of the bioprinting process. Lai-Fook and Hyatt<sup>51</sup> has previously shown that lung elasticity is dependent on the age of the person. It may be possible with our study to customize inhalers in order to maximize the delivery of costly medicines into the lungs via drop deposition. Lastly, there is a critical need in the agricultural industry to be able to efficiently spread and cover the surface area of plants with pesticides or fertilizers and these are often delivered by spray processes. By quantifying the relationship between the spreading factor  $\alpha$  and the elasticity E, we can determine the optimal impact velocity for pesticide application on a given plant to cover the leaves with the least amount of waste.

#### **■ SUBSTRATE PROPERTIES**

Substrates are prepared using the steps described above in different ratios of (i) base to cross-linker for PDMS silicone gels and (ii) mass ratio of gelatin powder to DI water for hydrogels. These different ratios give a range of materials properties, particularly stiffness, which we are interested in our experiments. Figure 10 plots the storage modulus and loss modulus for our substrates, as they depend upon these ratios.

# AUTHOR INFORMATION

### **Corresponding Author**

Joshua B. Bostwick — Department of Mechanical Engineering, Clemson University, Clemson, South Carolina 29634, United States; orcid.org/0000-0001-7573-2108; Phone: +1 (864) 656-5625; Email: jbostwi@clemson.edu

#### Author

Bailey C. Basso — Department of Mechanical Engineering, Clemson University, Clemson, South Carolina 29634, United States

Complete contact information is available at: https://pubs.acs.org/10.1021/acs.langmuir.0c02500

#### Notes

The authors declare no competing financial interest.

#### ACKNOWLEDGMENTS

J.B.B. acknowledges support from NSF Grant CBET-1750208.

### REFERENCES

(1) Worthington, A. M.; Cole, R. S. V. Impact with a liquid surface, studied by the aid of instantaneous photography. *Philosophical* 

- Transactions of the Royal Society of London. Series A, Containing Papers of a Mathematical or Physical Character 1897, 189, 137–148.
- (2) Pasandideh-Fard, M.; Qiao, Y.; Chandra, S.; Mostaghimi, J. Capillary effects during droplet impact on a solid surface. *Phys. Fluids* **1996**, *8*, 650–659.
- (3) Semenov, Y.; Wu, G.; Korobkin, A. Impact of liquids with different densities. *J. Fluid Mech.* **2015**, *766*, 5–27.
- (4) Mongruel, A.; Daru, V.; Feuillebois, F.; Tabakova, S. Early post-impact time dynamics of viscous drops onto a solid dry surface. *Phys. Fluids* **2009**, *21*, No. 032101.
- (5) Fukai, J.; Shiiba, Y.; Yamamoto, T.; Miyatake, O.; Poulikakos, D.; Megaridis, C. M.; Zhao, Z. Wetting effects on the spreading of a liquid droplet colliding with a flat surface: experiment and modeling. *Phys. Fluids* **1995**, *7*, 236–247.
- (6) Xu, L.; Nagel, S. R. Controlling the direction and amount of a splash with textured surface. *arXiv* **2007**, 0702098.
- (7) Alizadeh, A.; Bahadur, V.; Shang, W.; Zhu, Y.; Buckley, D.; Dhinojwala, A.; Sohal, M. Influence of substrate elasticity on droplet impact dynamics. *Langmuir* **2013**, 29, 4520–4524.
- (8) Gielen, M. V.; de Ruiter, R.; Snoeijer, J. H.; Gelderblom, H. Supressed splashing on elastic membranes. arXiv 2017, 1711.05634.
- (9) Pepper, R. E.; Courbin, L.; Stone, H. A. Splashing on elastic membranes: The importance of early-time dynamics. *Phys. Fluids* **2008**, 20, No. 082103.
- (10) Xu, L.; Barcos, L.; Nagel, S. R. Splashing of liquids: Interplay of surface roughness with surrounding gas. *Phys. Rev. E* **2007**, *76*, No. 066311.
- (11) van Dam, D. B.; Le Clerc, C. Experimental study of the impact of an ink-jet printed droplet on a solid substrate. *Phys. Fluids* **2004**, *16*, 3403–3414.
- (12) Gudapati, H.; Dey, M.; Ozbolat, I. A comprehensive review on droplet-based bioprinting: past, present and future. *Biomaterials* **2016**, 102. 20–42.
- (13) Cheng, Y.; Irshad, H.; Kuehl, P.; Holmes, T.; Sherwood, R.; Hobbs, C. Lung deposition of droplet aerosols in monkeys. *Inhalation Toxicol.* **2008**, 20, 1029–1036.
- (14) Hulse-Smith, L.; Illes, M. A blind trial evaluation of a crime scene methodology for deducing impact velocity and droplet size from circular bloodstains. *J. Forensic Sci.* **2007**, *52*, 65–69.
- (15) Rioboo, R.; Voué, M.; Adao, H.; Conti, J.; Vaillant, A.; Seveno, D.; De Coninck, J. Drop impact on soft surfaces: Beyond the static contact angles. *Langmuir* **2010**, *26*, 4873–4879.
- (16) Chen, L.; Li, Z. Bouncing droplets on nonsuperhydrophobic surfaces. *Phys. Rev. E* **2010**, *82*, No. 016308.
- (17) Chen, L.; Wu, J.; Li, Z.; Yao, S. Evolution of entrapped air under bouncing droplets on viscoelastic surfaces. *Colloids Surf.*, A **2011**, 384, 726–732.
- (18) Carré, A.; Gastel, J.-C.; Shanahan, M. E. Viscoelastic effects in the spreading of liquids. *Nature* **1996**, *379*, 432–434.
- (19) Mangili, S.; Antonini, C.; Marengo, M.; Amirfazli, A. Understanding the drop impact phenomenon on soft PDMS substrates. *Soft Matter* **2012**, *8*, 10045–10054.
- (20) Howland, C. J.; Antkowiak, A.; Castrejón-Pita, J. R.; Howison, S. D.; Oliver, J. M.; Style, R. W.; Castrejón-Pita, A. A. It's harder to splash on soft solids. *Phys. Rev. Lett.* **2016**, *117*, 184502.
- (21) Castillo-Orozco, E.; Davanlou, A.; Choudhury, P. K.; Kumar, R. Droplet impact on deep liquid pools: Rayleigh jet to formation of secondary droplets. *Phys. Rev. E* **2015**, *92*, No. 053022.
- (22) Thoroddsen, S. The ejecta sheet generated by the impact of a drop. *J. Fluid Mech.* **2002**, *451*, 373–381.
- (23) Weiss, D. A.; Yarin, A. L. Single drop impact onto liquid films: neck distortion, jetting, tiny bubble entrainment, and crown formation. *J. Fluid Mech.* **1999**, 385, 229–254.
- (24) Deegan, R.; Brunet, P.; Eggers, J. Complexities of splashing. *Nonlinearity* **2008**, *21*, C1.
- (25) Peregrine, D. The fascination of fluid mechanics. *J. Fluid Mech.* **1981**, *106*, 59–80.

- (26) Saylor, J. R.; Bounds, G. D. Experimental study of the role of the Weber and capillary numbers on Mesler entrainment. *AIChE J.* **2012**. *58*. 3841–3851.
- (27) Rein, M. Phenomena of liquid drop impact on solid and liquid surfaces. Fluid Dynamics Research 1993, 12, 61.
- (28) Lin, S.; Zhao, B.; Zou, S.; Guo, J.; Wei, Z.; Chen, L. Impact of viscous droplets on different wettable surfaces: Impact phenomena, the maximum spreading factor, spreading time and post-impact oscillation. *J. Colloid Interface Sci.* **2018**, *516*, 86–97.
- (29) Rioboo, R.; Tropea, C.; Marengo, M. Outcomes from a drop impact on solid surfaces. *Atomization Sprays* **2001**, *11*, 12.
- (30) Xu, L. Liquid drop splashing on smooth, rough, and textured surfaces. *Phys. Rev. E* **2007**, *75*, No. 056316.
- (31) Vega, E.; Castrejón-Pita, A. Suppressing prompt splash with polymer additives. *Exp. Fluids* **2017**, *58*, *57*.
- (32) Rioboo, R.; Marengo, M.; Tropea, C. Time evolution of liquid drop impact onto solid, dry surfaces. *Exp. Fluids* **2002**, 33, 112–124.
- (33) Style, R. W.; Wettlaufer, J. S.; Dufresne, E. R. Surface tension and the mechanics of liquid inclusions in compliant solids. *Soft Matter* **2015**, *11*, 672.
- (34) Mundo, C.; Sommerfeld, M.; Tropea, C. Droplet-wall collisions: experimental studies of the deformation and breakup process. *Int. J. Multiphase Flow* **1995**, *21*, 151–173.
- (35) Daniels, K. E.; Mukhopadhyay, S.; Houseworth, P. J.; Behringer, R. P. Instabilities in droplets spreading on gels. *Phys. Rev. Lett.* **2007**, *99*, 124501.
- (36) Spandagos, C.; Goudoulas, T. B.; Luckham, P. F.; Matar, O. K. Surface tension-induced gel fracture. Part 2. Fracture of gelatin gels. *Langmuir* **2012**, 28, 8017–8025.
- (37) Bostwick, J. B.; Daniels, K. E. Capillary fracture of soft gels. *Phys. Rev. E* **2013**, *88*, No. 042410.
- (38) Grzelka, M.; Bostwick, J. B.; Daniels, K. E. Capillary fracture of ultrasoft gels: variability and delayed nucleation. *Soft Matter* **2017**, *13*, 2962–2966.
- (39) Kittel, H. M.; Alam, E.; Roisman, I. V.; Tropea, C.; Gambaryan-Roisman, T. Splashing of a Newtonian drop impacted onto a solid substrate coated by a thin soft layer. *Colloids Surf., A* **2018**, 553, 89–96
- (40) Roisman, I. V. Inertia dominated drop collisions. II. An analytical solution of the Navier–Stokes equations for a spreading viscous film. *Phys. Fluids* **2009**, *21*, No. 052104.
- (41) Andrade, R.; Skurtys, O.; Osorio, F. Experimental study of drop impacts and spreading on epicarps: effect of fluid properties. *J. Food Eng.* **2012**, *109*, 430–437.
- (42) Dong, B.; Yan, Y.; Li, W. LBM simulation of viscous fingering phenomenon in immiscible displacement of two fluids in porous media. *Transp. Porous Media* **2011**, *88*, 293–314.
- (43) Bostwick, J. B.; Shearer, M.; Daniels, K. E. Elastocapillary deformations on partially-wetting substrates: rival contact-line models. *Soft Matter* **2014**, *10*, 7361–7369.
- (44) Karpitschka, S.; Das, S.; van Gorcum, M.; Perrin, H.; Andreotti, B.; Snoeijer, J. H. Droplets move over viscoelastic substrates by surfing a ridge. *Nat. Commun.* **2015**, *6*, 7891.
- (45) Park, S.; Bostwick, J.; De Andrade, V.; Je, J. Self-spreading of the wetting ridge during stick-slip on a viscoelastic surface. *Soft Matter* **2017**, *13*, 8331–8336.
- (46) Bayer, I. S.; Megaridis, C. M. Contact angle dynamics in droplets impacting on flat surfaces with different wetting characteristics. *J. Fluid Mech.* **2006**, *558*, 415.
- (47) Greenspan, H. P. On the motion of a small viscous droplet that wets a surface. *J. Fluid Mech.* **1978**, *84*, 125–143.
- (48) Rosenblat, S.; Davis, S. Frontiers in Fluid Mechanics; Springer, 1985; pp 171-183.
- (49) Bostwick, J. Spreading and bistability of droplets on differentially heated substrates. *J. Fluid Mech.* **2013**, 725, 566–587.
- (50) Stanley, C.; Jackson, R.; Karwa, N.; Rosengarten, G. The effects of surface wettability on droplet fingering. In *The Proceedings of the 19th Australasian Fluid Mechanics Conference*, Melbourne, Australia, December 8–11, 2014.

(51) Lai-Fook, S. J.; Hyatt, R. E. Effects of age on elastic moduli of human lungs. *J. Appl. Physiol.* **2000**, *89*, 163–168.